Supporting Information

Optimizing the photocatalytic properties of hydrothermal TiO_2 by the control of phase composition and particle morphology. A systematic approach.

Andrea Testino[a*], Ignazio Renato Bellobono[b], Vincenzo Buscaglia[c] Carmen Canevali[a], Massimiliano D'Arienzo[a], Stefano Polizzi[d], Roberto Scotti[a], and Franca Morazzoni[a]

[a] Department of Materials Science, University of Milano-Bicocca, Via R.Cozzi 53, I-20125 Milano, Italy

[b] Department of Physical Chemistry, Environmental Research Centre,University of Milano, Via Golgi 19, I-20133 Milano, Italy

[c] Institute for Energetics and Interphases, Dept. of Genova, National Research Council, Via De Marini, 6, I-16149, Genova, Italy

[d] Department of Physical Chemistry, University of Venezia, Via Torino 155/b, I-30172 Venezia, Italy

[*] Corresponding author. E-mail: andrea.testino@mater.unimib.it

Contents

Scheme S1. Relevant equilibria in the TiO_2-H_2O-HCl-NH_3 system. In the reactions, the H_2O molecules are not reported as ligands in the Ti complexes. These have to be considered as octahedrally coordinated, e.g. $[Ti(Cl)_3(H_2O)_3]^+$ instead of $TiCl_3^+$.

1. $TiOCl_2(aq) + 3H_2O \rightarrow Ti(OH)_4(aq) + 2HCl(aq)$
2. $TiO_2(s) + OH^- \rightleftarrows HTiO_3^-$
3. $Ti(OH)_4(aq) \rightleftarrows TiO_2(s) + 2H_2O$
4. $Ti^{4+} + H_2O \rightleftarrows Ti(OH)^{3+} + H^+$
5. $Ti(OH)^{3+} + H_2O \rightleftarrows Ti(OH)_2^{2+} + H^+$
6. $Ti(OH)_2^{2+} + H_2O \rightleftarrows Ti(OH)_3^{+} + H^+$
7. $Ti(OH)_3^{+} + H_2O \rightleftarrows Ti(OH)_4(aq) + H^+$
8. $Ti^{4+} + Cl^- \rightleftarrows TiCl^{3+}$
9. $TiCl^{3+} + Cl^- \rightleftarrows TiCl_2^{2+}$
10. $TiCl_2^{2+} + Cl^- \rightleftarrows TiCl_3^{+}$
11. $TiCl_3^{+} + Cl^- \rightleftarrows TiCl_4(aq)$
12. $TiCl_4(g) \rightleftarrows TiCl_4(aq)$
13. $NH_3(g) \rightleftarrows NH_3(aq)$
14. $NH_3(aq) + H_2O \rightleftarrows NH_4^+ + OH^-$
15. $H^+ + OH^- \rightleftarrows H_2O$
16. $HCl(g) \rightleftarrows HCl(aq)$
17. $HCl(aq) \rightleftarrows H^+ + Cl^-$
18. $H_2O(g) \rightleftarrows H_2O$

Table S1. Relevant species in the TiO_2-H_2O-HCl-NH_3 system and corresponding standard state properties at 298.15 K [36]

	Ionic species											
	H^+	OH^-	NH_4^+	Cl^-	Ti^{4+}	$TiCl^{3+}$	$TiCl_2^{2+}$	$TiCl_3^+$	$TiOH^{3+}$	$Ti(OH)_2^{2+}$	$Ti(OH)_3^+$	$HTiO_3^-$
ΔG° (J mol^{-1}) 10^{-4}	0	-15.7	-7.95	-13.1	-35.4	-44.5	-58.7	-72.7	-61.4	-87.0	-109	-95.6
ΔH° (J mol^{-1}) 10^{-5}	0	-2.30	-1.33	-1.67	-4.22	-5.58	-7.45	-9.47	-6.71	-9.52	-12.2	-10.4
S° (J mol^{-1} K^{-1}) 10^{-1}	0	-1.07	11.1	5.67	-45.6	-43.5	-41.0	-43.9	-19.0	-4.08	5.69	11.7
C°p (J mol^{-1} K^{-1}) 10^{-1}	0	-13.7	6.59	-12.3	98.7	54.9	108	157	-32.2	-105	-153	-10.6
V° 10^6 (m^3 mol^{-1})	0	-4.18	18.1	17.8	-10.4	-38.0	-17.9	5.40	-6.52	-3.77	-1.51	-2.21

	Aqueous species					Gaseous species				Solid species
	H_2O	$Ti(OH)_4$	NH_3	$TiCl_4$	HCl	HCl	H_2O	NH_3	$TiCl_4$	TiO_2 (anatase)
ΔG° (J mol^{-1}) 10^{-4}	-23.7	-132	-2.67	-86.7	-9.51	-9.53	-22.9	-1.65	-72.6	-88.3
ΔH° (J mol^{-1}) 10^{-4}	-28.6	-151	-8.13	-117	-11.6	-9.23	-24.2	-4.61	-76.3	-93.9
S° (J mol^{-1} K^{-1}) 10^{-1}	7.00	5.48	10.8	-53.6	10.5	18.7	18.9	19.2	35.3	4.99
C°p (J mol^{-1} K^{-1}) 10^{-1}	7.53	5.02	7.49	201	-3.18	2.91	3.36	3.56	9.54	5.53
V° 10^6 (m^3 mol^{-1})	18.1	-.350	24.4	32.9	0	-	-	-	-	20.5
a (J mol^{-1} K^{-1})	-	-	-	-	-	-	-	-	-	69.9
b 10^3 (J mol^{-1} K^{-2})	-	-	-	-	-	-	-	-	-	8.54
c 10^{-5} (J mol^{-1} K)	-	-	-	-	-	-	-	-	-	-15.3

Table S2. Summary of hydrothermal synthesis experiments and properties of the corresponding titania powders.

Sample(1)	**Synthesis conditions**(2)			**Anatase**			**Rutile**			**Brookite**			**density**		**Specific surface**		**Pores**
ID	V_A	t_R	T_R	Wt.	d (101)	α(3)	Wt.	d (110)	α(3)	Wt.	d (211)	α(3)	XRD(4)	ρ(5)	XRD(6)	BET	BJH DPV(7)
	(ml)	(h)	(°C)	%	(nm)	(-)	%	(nm)	(-)	%	(nm)	(-)	(g cm^{-3})		(m^2 g^{-1})		(ml g^{-1})
S0	0-50	0.17	85	>90	<5		<5	<5		<5	<5						
S2 [1]	5	2	220	57	15.8		43	47		-							
S3 [1]	12	2	220	65	14.6		35	53		-			4.01	3.89		68	0.41
S12 [1]	45	2	220	98	9.5		0	-		2	n.d.		3.81	3.76		129	0.59
S13 [1]	42	2	220	56	10.5		1	n.d.		43	10.0		4.00	3.91		88	0.51
S141 [3]	20	2	220	20	13.1	1	78	73	5	2	n.d.	1	4.18	4.05	45	46	
S142 [1]	20	1.5	220	30	12.7		67	80		3	10.7		4.14	4.08			
S143 [3]	20	2	161	57	9.9		14	22		29	10.0						
S15 [1]	20	1	220	48	12.5		38	46		13	16.7		4.02	3.97		71	0.34
S16 [1]	20	6	220	-	-	-	100	108	3	-			4.24	4.24	10	11	0.03(8)
S17 [1]	0	2	220	52	14.3	2	48	26	5	-		2	4.06	3.91	66	64	
S18 [2]	10	2	220	67	15.7	3	30	35	5	3	12.0	3	3.97	3.85	73	68	
S19 [1]	50	6	220	98	15.9		0	-		2	n.d.			3.81			
S20(9) [1]	-	-	-	100	22.5		0	-		-				3.82			
S21 [1]	0	6	220	43	14.9		57	31		-				3.99			
S22 [1]	50	2	220	95	14.9	1	0	-		5	n.d.	1	3.90	3.80	98	91	
S23 [1]	50	1	220	95	14.6		0	-		5	n.d.			3.80			
S25 [1]	40	2	161	45	10.2		3	21		52	10.2			3.93			
S26 [1]	20	2	109	48	11.2		14	22		37	10.6			3.93			
S27 [1]	20	2	132	51	11.2		12	21		37	10.2		4.02	3.90		91	
S28 [1]	20	2	184	45	13.2		31	31		23	11.1			3.95			
S33 [1]	15	2	161	64	10.2		17	22		19	9.3						
S34 [1]	25	2	161	53	9.4		17	22		30	9.1						
S35 [1]	35	2	161	45	9.7		14	20		41	9.5						
S361 [1]	10	2	161	67	11.1		23	24		10	10.0		4.00	3.86		94	
S371 [2]	30	2	220	-	-	-	100	58	5	-			4.24	4.20	18	20	
S38 [1]	15	2	220	36	13.9		61	68		3	n.d.						
S40 [1]	25	2	220	-	-	-	100	66		-							
S411 [1]	20	2	250	3	n.d.		97	87		-							
S412 [2]	35	2	220	13	10.8	3	76	80	5	11	17.2	3			32		
S42 [1]	40	2	220	45	10.1	3	18	71	5	37	10.6	3	4.05	3.96		88	
P25	-	-	-	77	23		23	37.5		-						54	0.14

(1) The number in square brackets is the number of repetitions of the experiments. The reported data in the arrow are the mean value.
(2) V_A: volume of ammonia solution; t_R: reaction time; T_R: reaction temperature.
(3) Aspect ratio, α=length/width, estimated from TEM images.
(4) Density calculated from Rietveld refinement of the XRD patterns.
(5) Experimental density from He pycnometry
(6) Calculated from composition, crystallite size and α for each phase.
(7) BJH Desorption Pore Volume
(8) Non-mesoporous material (Type 2 isotherm)
(9) Obtained treating sample S12 at 550°C for 10h

Table S3. Photocatalytic properties of selected titania samples.

Sample	$(dC/dt)_{max}$ (1)	$t_{1/2}$ (2)	Mean Crystallite size (3)	Relative Mineralization Rate(4)	Specific Surface Area
	(ppm/min)	(min)	(nm)	(-)	(m^2 g^{-1})
Blank	1.81	55	-	*0*	-
Degussa P25	2.66	28	26	*1*	54
S2T	3.08	29	29	1.5	
S3T	2.76	35	28	1.1	68
S12T	2.37	39	9	0.7	129
S13T	2.09	43	10	0.3	88
S141T	3.66	24	62	2.2	46
S142T	3.45	25	58	1.9	
S15T	3.04	31	26	1.4	71
S16H	4.83	18	108	3.5	11
S16HT	4.07	21	108	2.6	11
S17T	2.46	39	20	0.8	64
S18T	2.80	33	17	1.2	68
S19T	2.46	41	16	0.8	
S20TT(5)	2.80	33	23	1.2	
S21T	2.44	27	24	0.7	
S22T	2.38	40	14	0.7	91
S23T	2.32	43	14	0.6	
S24T	2.27	39	23	0.5	
S371H	4.60	19	58	3.3	20
S371	3.89	22	50	2.4	
S40T	3.94	23	70	2.5	
S411H	3.88	24	85	2.4	
S411HT	3.58	25	85	2.1	

(1) Calculated as shown in Figure 13. Standard error 0.2 ppm/min

(2) Calculated as shown in Figure 13. Standard error 3 min

(3) Calculated as weighted mean value of the crystallite size (XRD) of the different polymorphs.

(4) Calculated by setting 0 for blank and 1 for Degussa P25

(5) Obtained treating sample S12 at 550°C for 10h

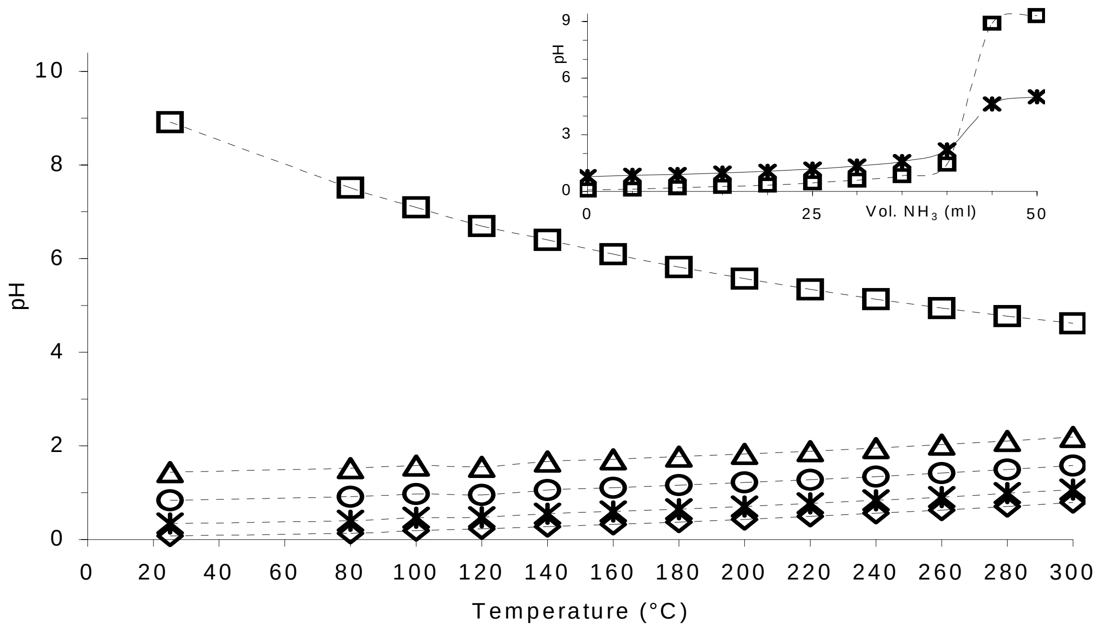

Figure S1. pH as a function of temperature under hydrothermal conditions calculated for an overall Ti concentration of 0.45 mol/kg and different ammonia solution volumes (□: 45 ml; △: 40 ml; ○: 35 ml; ∗: 20 ml; ◇: 0 ml). Inset: pH as a function of ammonia solution volume for different temperatures (□: 25 °C; ∗:300 °C).

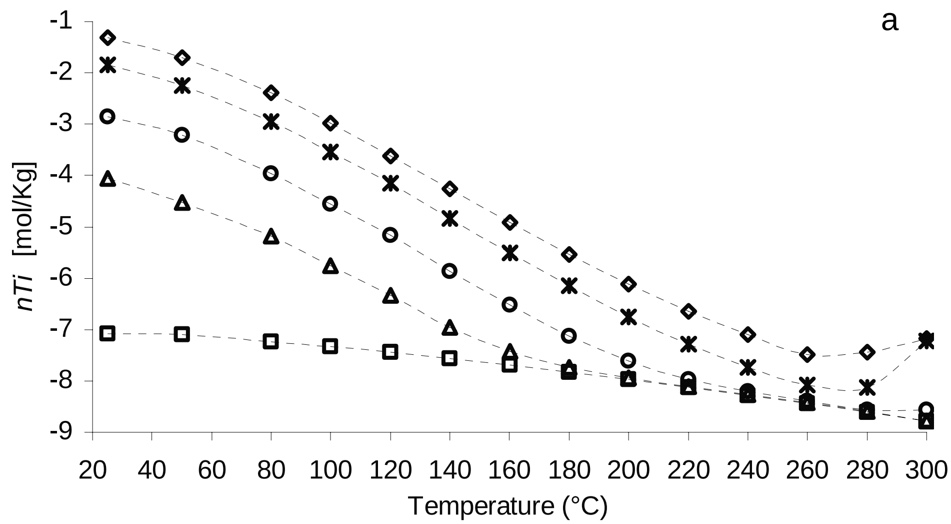

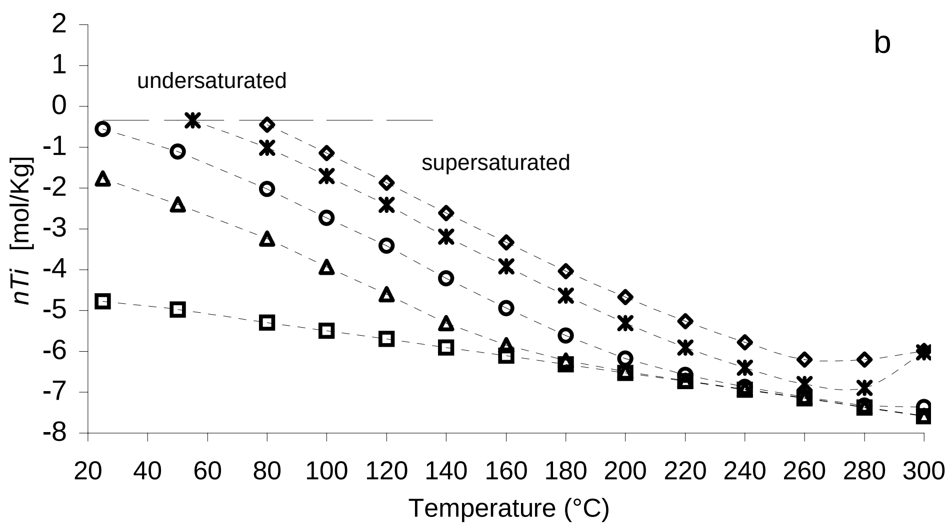

Figure S2. Solubility of TiO_2 as a function of temperature under hydrothermal conditions calculated for an overall Ti concentration of 0.45 mol/kg and different ammonia solution volume (□: 45 ml; △: 40 ml; ○: 35 ml; ∗: 20 ml; ◇: 0 ml). (a) Influence of particle size neglected. (b) Calculated for 12 nm particles (γ = 0.5 J m^{-2}). The horizontal line in (b) denotes n_{Ti} = 0.45 mol/kg. The quantity n_{Ti} plotted on the y-axis represents the overall amount (mol/Kg) of titanium in solution and takes into account all the aqueous species. The solubility curves in Fig S2b were calculated using the Gibbs-Thompson equation

$$\ln \frac{K_{s,d}}{K_s} = 4 \frac{\nu \gamma_{l,s}}{k_B T \, d}$$

where K_s is the solubility constant of a macroscopic crystal, $K_{s,d}$ is the solubility constant of a crystal with diameter d, ν is the unit cell volume, γ is the liquid-solid surface energy, T the temperature and k_B

the Boltzmann constant. The dashed horizontal line in Fig. S2b corresponds to a concentration of 0.45 mol/kg. This line meets the curve V_A = 0 ml at T≈80°C. Experimentally, it has been observed that a clear 0.45 mol/kg solution, when heated from room temperature to 100 °C, produces a precipitation of anatase nanocrystals starting at 80-85°C in 1-3 minutes, in agreement with the calculations

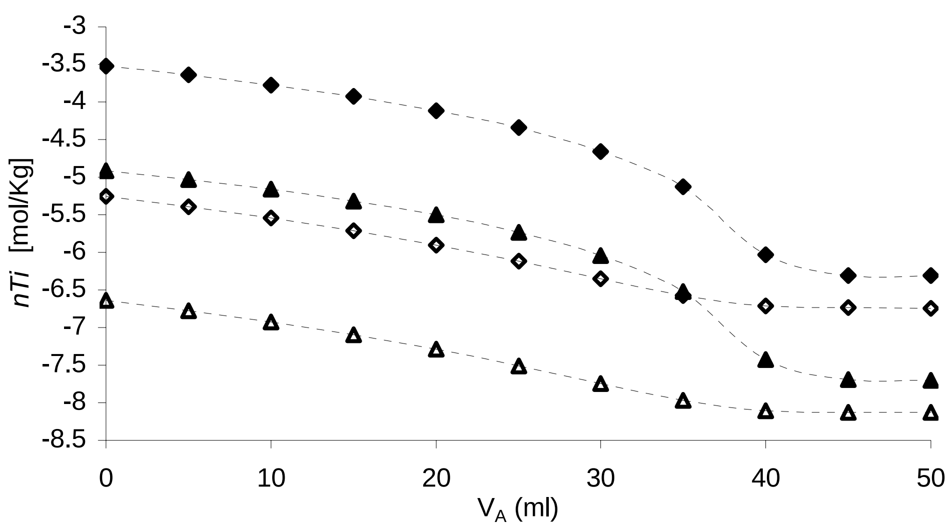

Figure S3. Solubility of TiO_2 as a function of the volume of ammonia solution under hydrothermal conditions calculated for an overall Ti concentration of 0.45 mol/kg (△: macroscopic crystal, T=220 °C; ▲: macroscopic crystal , T=160 °C; ◇: particle diameter 12 nm, T=220 °C; ◆: particle diameter 12 nm, T=160 °C). The quantity n_{Ti} plotted on the y-axis represents the overall amount (mol/Kg) of titanium in solution and takes into account all the aqueous species.

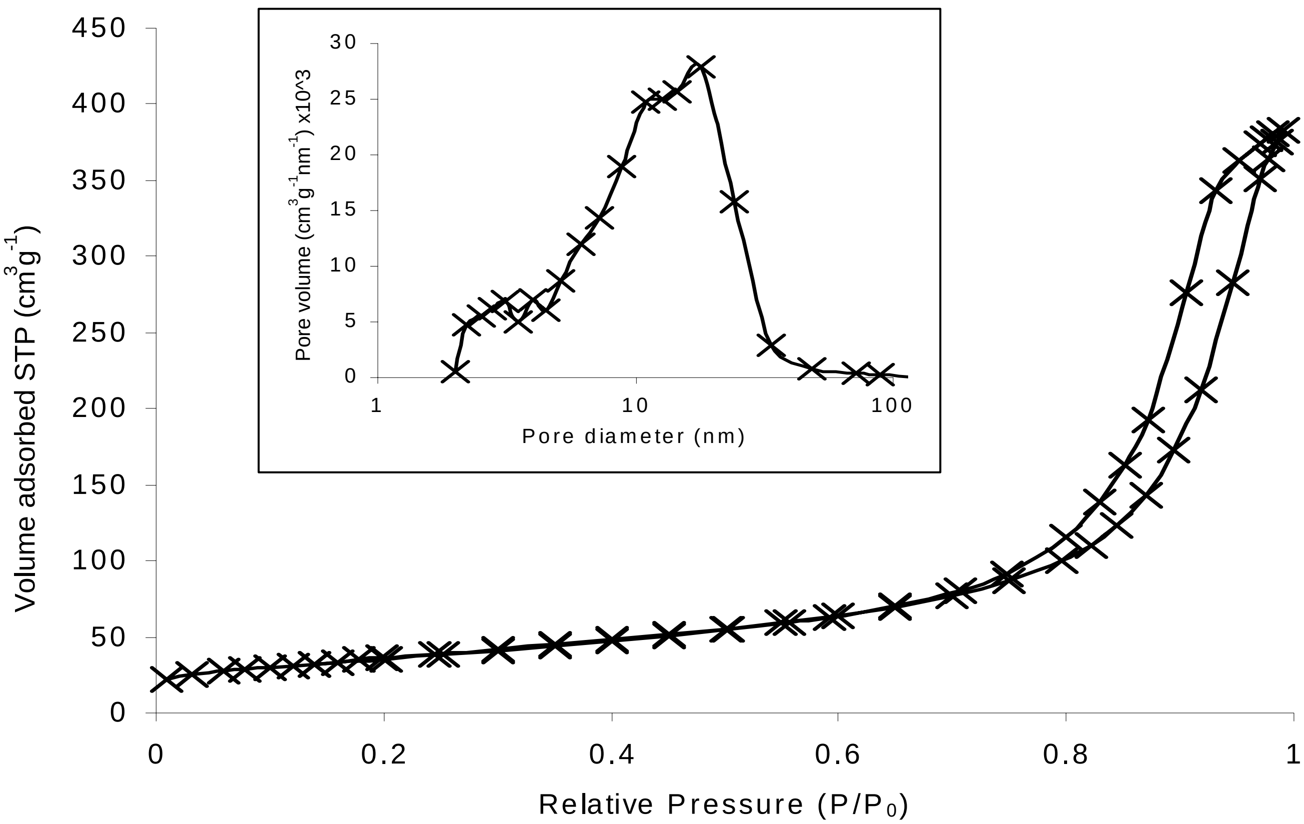

Figure S4. Adsorption/desorption isotherm at liquid nitrogen for sample S12T. The curves correspond to a type IV isotherm with capillary condensation in the mesopores. Inset: pore size distribution.

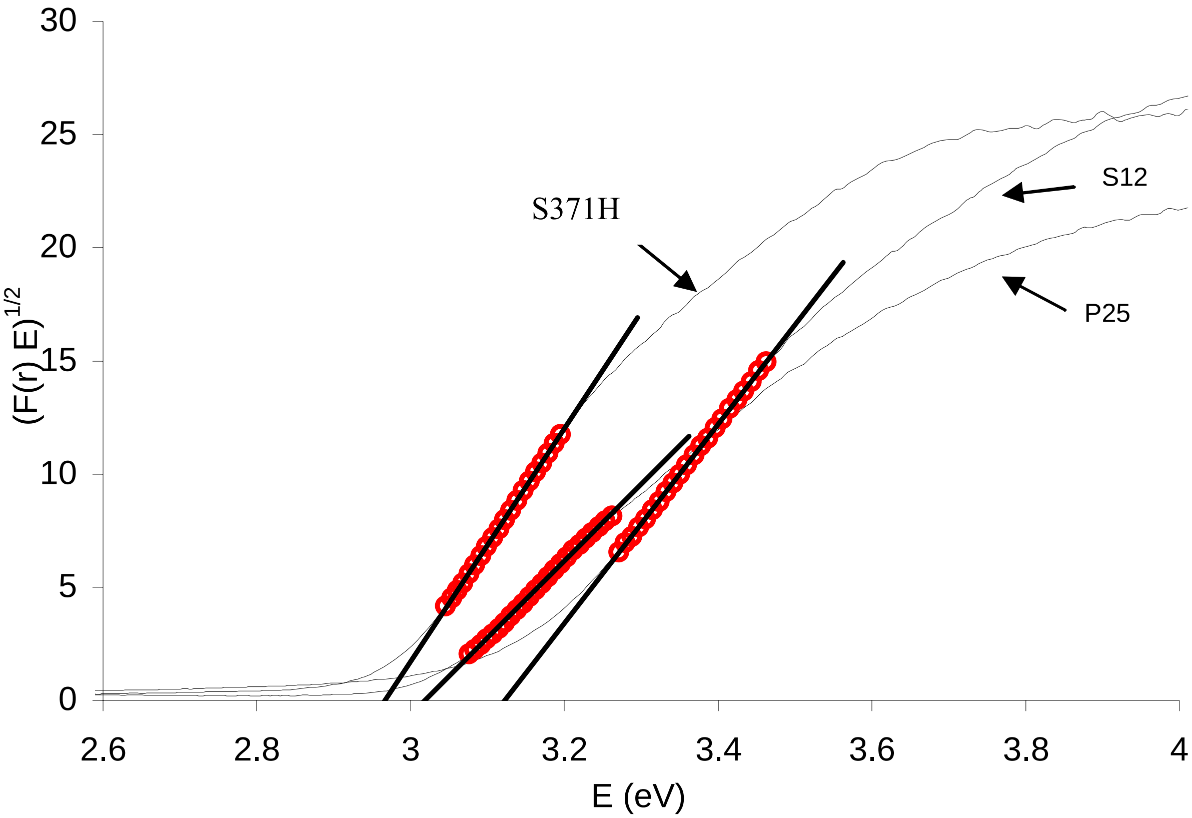

Figure S5. Tauc plot for samples S12 (100% A), S371H (100% R) and Degussa P25. The band gap is evaluated from the intercept with the energy axis of the straight line fitted to the linear portion of the curve.